Conceptual Design of a Wheel-Based Energy Harvesting Device for Low-Speed Driving and Vehicle Acceleration/Deceleration

[1]Eun June Lee, [2]Hyun Min Park, [3]Jung Woo Kim Park
[1,2]Department of Mechanical Engineering, Gaon Highschool, Gyeonggi-do, Republic of Korea

[1]Corresponding Author: eunjune1208@gmail.com

Keywords: Energy Harvesting, Electromagnetic system, Automobiles, Wheel, Arduino Circuit, Current Measurement

Abstract

In this study, we analyzed previous studies on automotive wheel energy harvesters using piezoelectric methods and designed and analyzed a low-speed energy harvester that can be mounted inside the spokes using electromagnetic induction. Through mathematical analysis, we theoretically confirmed the potential for power generation. In an actual experiment, by connecting five generators in parallel within five spokes, results of 1.3A, 1.56V, and 2.028W are obtained. Based on these results, the difference from the calculated value and its causes are analyzed, and an improved study of addressing the problems is proposed. It is confirmed that the power output at low speeds is higher than that of previous small piezoelectric energy harvesters. Thus, it is concluded that it can be applied in combination with other generators.

1. Introduction

Recently, due to environmental pollution and depletion of fossil fuels, renewable energy is receiving increasing attention as an alternative. Along with the development and advancement of renewable energies such as solar thermal, solar photovoltaic, wind, and hydroelectric power, their limitations have also become apparent [1]. Based on these limitations, research on energy harvesting has been actively conducted to address issues of efficiency and intermittency in renewable energy. Technologies have been developed and studied to convert various forms of wasted energy, such as regenerative braking, heat [2], vibration [3,4], and other kinetic energies [5], into usable forms.

In line with this interest in energy generation, technologies to collect wasted energy inside automobiles beyond regenerative braking have also been developed. In particular, research has been conducted to convert vibrations from suspensions into electrical energy, simultaneously aiming for both power generation and improved stability [6]. As part of automotive energy harvesting that can be applied alongside such technologies, this study proposes a method to convert energy generated from the rotational force of car wheels into electricity.

2. Analysis of Previous Research

In the study “HARVESTING ENERGY FROM VEHICLE WHEELS” by G. Manla, N. M. White, and J. Tudor, a system using a piezoelectric generator to obtain electricity from rotating vehicle wheels was utilized. This method generates electricity by applying impact to the piezoelectric element using the centrifugal force of the wheel. In the study, the generator was attached to the wheel rim, and 4mW of power was produced at 800 rpm using a test wheel with a diameter of 0.12 m [7].
In the study “Piezoelectric Energy Harvesting from Automotive Wheels” by Vaishak, Roopa Manjunatha, and G. L. Manjunath, an energy harvester based on a piezoelectric sensor was installed inside the wheel spokes, used to charge a lead-acid battery. Using MATLAB, it was confirmed that the device operates within the 20~120 km/h speed range, and it was demonstrated that sufficient power can be harvested at speeds over 60 km/h to charge a 12V lead-acid battery [8].

Unlike previous studies that adopted power generation methods using piezoelectric elements, this study focused on electromagnetic induction and designed the generator. Five coils are placed inside the wheel spoke, and the magnets move through the coils. When the car accelerates or decelerates and passes the angular velocity point where centrifugal force and gravity balance within the wheel magnet, the magnet moves through the coil, generating current as the primary power source. Additionally, vibrations from road surfaces and the wheel’s rotation transform the relative position of the magnet and coil, inducing differneces in magnetic flux through the coil, which generates electricity.

3. Design of Experiment

In this study, the vehicle wheel is assumed to have five spokes, and the generator is designed with a coil and magnet located inside each spoke. The wheel’s outer diameter was set to 201 mm, the rim thickness to 4 mm, the hub to an outer diameter of 58.606 mm, and an inner diameter of 54.606 mm. The spokes were designed as cylinders with a diameter of 31.5 mm, and five spokes were evenly arranged at equally spaced angles.

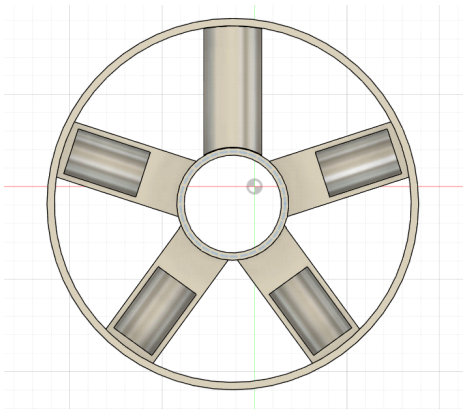

Figure.1 Energy harvester 3D model.

The space for the internal coil in the spoke is a cylinder with a diameter of 25.5 mm and a length of 41 mm. The base of the cylinder, which is the closest part of the cylinder to the hub, is located 53 mm from the hub’s center, and the vertical axis aligns with the spoke center. The spoke is divided vertically in half, allowing the coil and magnet to be placed inside and sealed afterward.

To rotate the wheel and measure the energy output, a motor and measurement devices are attached to the hub. In front of the hub, a motor is fixed to make rotational motion. On the opposite side, an Arduino, a current sensor, a Bluetooth module for data transmission, and batteries are equipped. The five coils inside the five spokes are connected in parallel, and diodes are used to ensure unidirectional current

flow, preventing current cancellation between two or more reversed coils. A resistor and a current sensor are inserted in the middle of the electric wire. A discrete Arduino is set for the motor.

4. Numerical Analysis of Experiment

In this study, the energy harvester operates on the law of electromagnetic induction. In electromagnetic induction, the induced electromotive force can be expressed as follows.

$$\varepsilon = -N\frac{d\Phi}{dt} \tag{1}$$

In the above equation, N denotes the number of turns of the coils, Φ represents the magnetic flux, and the induced electromotive force is expressed as the product of the number of coil turns and the time derivative of the magnetic flux. Magnetic flux can be expressed as follows.

$$\Phi = B \cdot A \cdot \cos\theta \tag{2}$$

The magnetic flux can be expressed as the product of the magnetic field, the cross-sectional area of the coil, and the cosine of the angle between the area vector and the magnetic field. In this study, the angle between the magnet and the coil is assumed as 180°. Thus, the value of $\cos\theta$ remains equal to 1. In the above equation, B, representing the magnetic field, can be expressed as follows.

$$B = \frac{\mu_0 M}{2}\left(\frac{x+L}{\sqrt{(x+L)^2+R^2}} - \frac{x-L}{\sqrt{(x-L)^2+R^2}}\right) \tag{3}$$

M denotes the magnetization of the magnet. In this study, the magnetization of the neodymium magnet is $1.15\times10^6 A/m$. L and R represent the length of the magnet and the radius of its cross-section, with values of 0.01m and 0.005m.

$$\frac{d\Phi}{dt} = A \cdot \frac{dB}{dt} \tag{4}$$

The time derivative of the magnetic flux can be represented as follows. Since the cross-sectional area A is a constant, it is not affected by time.

The time derivative of the magnetic field can be obtained through the following calculation process. For the convenience of calculating, B is expressed as $f(x)$ and $g(x)$.

$$f(x) = \frac{x+0.01}{\sqrt{(x+0.01)^2+0.005^2}} \tag{5}$$

$$g(x) = \frac{x-0.01}{\sqrt{(x-0.01)^2+0.005^2}} \tag{6}$$

$$\frac{dB}{dt} = \frac{dB}{dx} \cdot \frac{dx}{dt} \tag{7}$$

$$\frac{dB}{dt} = \frac{\mu_0 M}{2}\left(\frac{d}{dx}f(x) - \frac{d}{dx}g(x)\right) \cdot \frac{dx}{dt} \tag{8}$$

In this study, the determination of the magnet‘s velocity requires consideration of both the centrifugal force and the gravitational force acting upon the magnet. For this purpose, basic information about the angular velocity and the angle of the wheel is necessary. The motor, which makes the rotational motion of the

wheel, requires 0.7 seconds to reach a rotational speed of 95 rpm. It can be assumed as a linear function over time. Since 95 rpm corresponds to 10 rad/s, the angular velocity can be expressed as follows.

$$\omega(t) = \frac{100}{7}t \tag{9}$$

이하 AI 검사 시행 X, 표절검사 시행 O

Integrating this expression with respect to time yields the equation for angular displacement, as shown below.

$$\theta(t) = \int_0^t \frac{100}{7} k dk = \frac{50}{7}t^2 \tag{10}$$

The centrifugal force can be expressed by the following equation.

$$F_{centrifugal} = m \cdot \omega^2 \cdot r \tag{11}$$

And, the gravitational force can be represented as follows.

$$F_{gravity} = m \cdot g \cdot \sin\theta \tag{12}$$

The radius of the designed energy harvester is approximately 0.1m, and the mass of the magnet is about 50g. Based on these parameters, the forces acting on the magnet can be summarized as follows.

$$F_{magnet} = 50 \times 10 \times \sin\theta - 50 \times \omega^2 \times 0.1 \tag{13}$$

By substituting the measured quantities and the results of Eqs. 8 and 9 into the preceding expression, we obtain the following.

$$F_{magnet} = 500 \times \sin\frac{50}{7}t^2 - 5 \times \frac{10000}{47}t^2 \tag{14}$$

The acceleration of the magnet, obtained by dividing the above expression by the mass of the magnet, is given as follows.

$$a = 10 \times \sin\frac{50}{7}t^2 - \frac{1000}{47}t^2 \tag{15}$$

The initial velocity of the magnet is 0, the velocity over time is as follows.

$$v = 10 \cdot t \cdot \sin\frac{50}{7}t^2 - \frac{1000}{47}t^3 \tag{16}$$

The displacement of the magnet can be expressed as follows.

$$\Delta x = 10 \cdot t^2 \cdot \sin\frac{50}{7}t^2 - \frac{1000}{47}t^4 \tag{17}$$

Since the initial velocity of the magnet is zero, its velocity as a function of time can be expressed as follows.

$$x = 0.005 - \Delta x \tag{18}$$

According to Eqs. 8 and 18, the graph of the time derivative of the induced magnetic field is illustrated as follows.

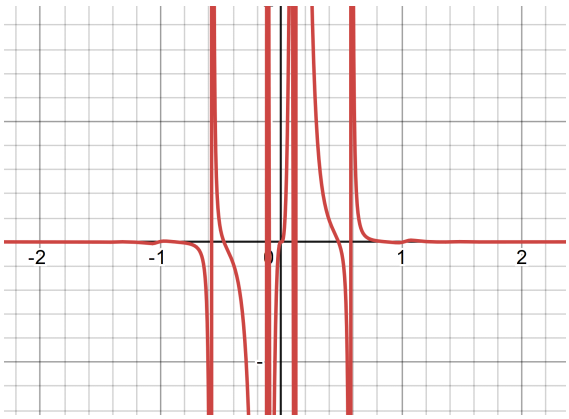

Figure.2 $\frac{dB}{dt}$ graph in t-B plane.

The graph of the time derivative of the magnetic flux, obtained by multiplying A in Fig.2, is shown as follows.

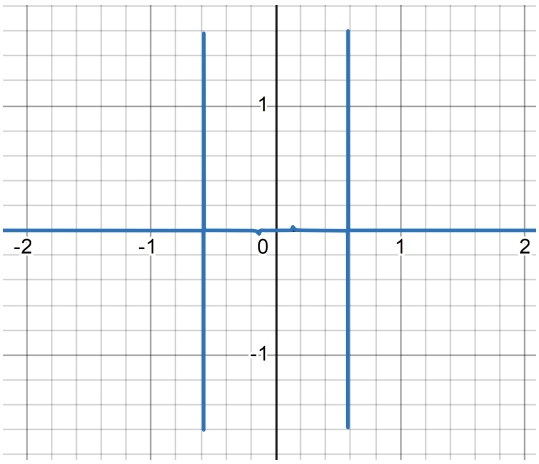

Figure.3 $\frac{d\Phi}{dt}$ graph in t-Φ plane.

The time interval considered in this study is [0,0.5], and the corresponding graph of the time derivative of the magnetic flux within this range is presented in Fig.4.

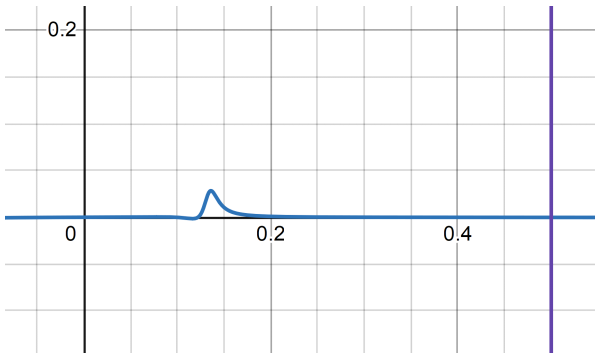

Figure.4 $\frac{d\Phi}{dt}$ graph in t-Φ plane (t: 0~0.5).

Within this interval, the maximum value of the time derivative of the magnetic flux is approximately 0.0285 V. According to Eq. (1), the maximum induced electromotive force within this range is given as follows.

$$\varepsilon_{\max} = -300 \times 0.0285\,V = 8.55\,V \qquad (19)$$

Therefore, the expected voltage value of this experiment is 8.55 V.

5. Fabricating of Energy Harvester

The wheel was fabricated by 3D printing, consisting of five spoke covers and one main body. The interior of the hub was printed completely hollow to ensure that the subsequent attachment of the motor would not be obstructed. For the motor, an Arduino DC motor designed for RC cars was employed. It was connected to the Arduino wheel and mounted inside the hub of the fabricated wheel to secure it in place. Photographs of the motor and wheel used are shown below.

Figure.5 Arduino DC motor and wheel.

The DC motor was powered through the Arduino, which in turn was supplied by a battery equipped with an on/off function to facilitate convenient control of the wheel's operation. During the experimental procedure, the Arduino, battery, and motor were securely fixed to prevent any movement. A simplified schematic diagram of the circuit employed in this study to measure the energy recovery efficiency is shown below.

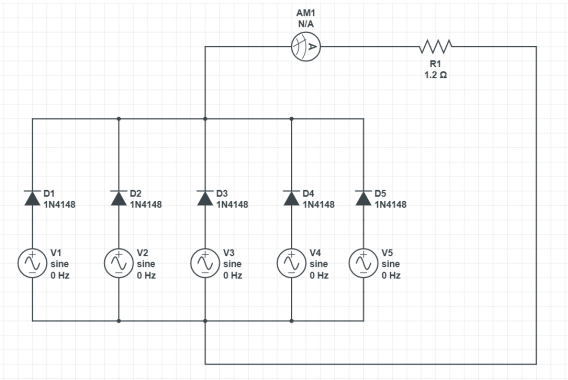

Figure.6 Circuit diagram of energy harvester.

In the circuit diagram of Fig. 3, the coil is represented as an alternating voltage source, while the current sensor is depicted as an ammeter. The current induced in the coil is rectified through a diode, allowing only current in a specific direction to pass, after which it flows through the current sensor and resistor before returning to the coil.

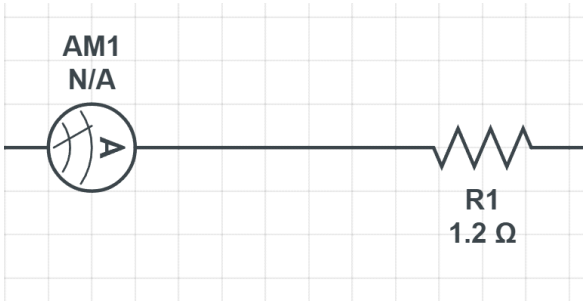

Figure.7 Resister and current sensor.

In this study, resistors of 1.2 Ω, 220 Ω, and 10 kΩ were employed in the experiments, and based on the accuracy and reliability of the results obtained, the use of a 1.2 Ω resistor was determined to be the most appropriate. Finally, a photograph of the actual generator fabricated on the basis of this circuit diagram is shown below.

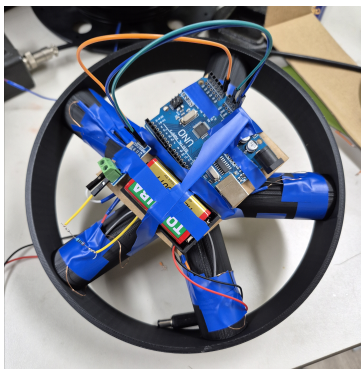

Figure.8 Energy harvester (1).

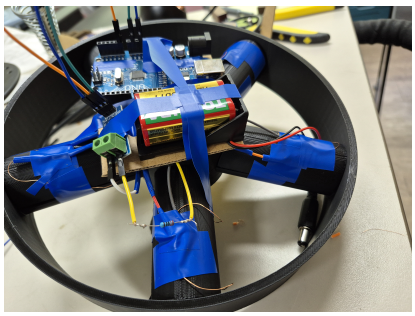

Figure.9 Energy harvester (2).

6. Analysis of Experiment Result

In this chapter, the process of selecting the resistor with the highest accuracy and reliability

among 1.2 Ω, 220 Ω, and 10 kΩ, as well as analyzing the experimental results to derive the generated power, is addressed. In the experimental results, an issue arose in which the measured current did not yield 0 A when the generator was inactive (i.e., when the generated power was zero). Therefore, calculations for voltage and power were performed using V, which is defined as follows.

$$\Delta I = |I_{\max} - I_{\min}| \tag{20}$$

Here, $I_{\min}$ denotes both the minimum value of the current and the mode of the measured current when the generator is in an inactive state. A portion of the experimental data obtained using the 10 kΩ resistor is presented below.

Table.1 10kΩ current data.

Current [A]
-0.15
-0.12
-0.15
0.62
0.30
0.38
0.78
0.12
0.57
0.75
1.23
0.78
2.66
2.79

Here, the maximum current is 2.79 A and the modal value in the inactive state is -0.15 A; therefore, for the 10 kΩ case, ΔI is given as follows.

$$\Delta I = 2.79A - (-0.15A) = 2.94A \tag{21}$$

The voltage computed from the resistance and current is as follows.

$$V = IR = 29.4kV = 29{,}400\,V \tag{22}$$

On this basis, the power is obtained as follows.

$$P = VI = 86{,}436\,W \tag{23}$$

These values are excessively large for the generator fabricated in this study; had such voltage and current actually been produced, issues such as overheating or mechanical failure would likely have occurred. Accordingly, the 10 kΩ case can be excluded from consideration. A subset of the experimental data obtained using the 220 kΩ resistor is presented below.

Table.2 220Ω current data.

Current [A]
-0.73
-0.81
-0.81
-0.78
-0.91
-0.89
-0.99
-1.07
-1.31
-1.31
-1.33

In Table 2, the minimum current is -1.33 A and the maximum current is -0.73 A. Accordingly, ΔI is given as follows.

$$\Delta I = |-1.33A - (-0.73A)| = 0.6A \tag{24}$$

Using the foregoing information, the voltage

is computed as follows.

$$V = IR = 0.6A \times 220\Omega = 132\,V \quad (25)$$

On this basis, the power is obtained as follows.

$$P = VI = 79.2\,W \quad (26)$$

A voltage of 132 V and a power of 79.2 W are values attainable with precision generators; however, in energy-harvesting environments such as the present study, such magnitudes are unlikely. Therefore, the 220 Ω case can be excluded from consideration, and the 1.2 Ω resistor is selected.

Among the data obtained with the 1.2 Ω resistor, the maximum and minimum currents are −0.03 A and −1.33 A, respectively. Based on these values, ΔI is calculated as follows.

$$\Delta I = |-0.03A - (-1.33A)| = 1.3A \quad (27)$$

The corresponding voltage and power are then given as follows.

$$V = IR = 1.56\,V \quad (28)$$

$$P = VI = 2.028\,W \quad (29)$$

These values constitute reasonable voltage and power levels for an energy-harvesting generator based on electromagnetic induction.

7. Conclusion and Recommendations

7.1. Comparison with Expectation and Previous Researches

In prior studies employing piezoelectric methods, peak power output typically remained at the level of several tens of milliwatts or a few milliwatts [7, 9-11]. In contrast, by adopting electromagnetic induction and a structure in which multiple generators are connected in parallel, the present study achieved a peak power of approximately 2.03 W and peak voltage and current of 1.56 V and 1.3 A, respectively. These values are substantially higher than those reported for typical small-scale piezoelectric generators.

By contrast, the generator fabricated in this work is not intended for continuous power generation; rather, the circumstances under which generation occurs can be described by the following equations.

$$F = mg \quad (30)$$

Here, F denotes the centrifugal force and can be expressed as follows.

$$F = m \cdot \omega^2 \cdot r = \frac{mv^2}{r} \quad (31)$$

Accordingly, the threshold angular velocity at which power generation occurs in the tire is given by following equation.

$$\omega = \sqrt{\frac{g}{r}} \quad (32)$$

On this basis, letting Δω represent the difference between the threshold angular velocity and the current angular velocity, the condition for power generation can be expressed as follows.

$$\Delta\omega = \omega_{current} - \omega = \omega_{current} - \sqrt{\frac{g}{r}} \quad (33)$$

From Eq. (33), power generation is defined as occurring when the sign of $\Delta\omega$ is negative. Thus, power is generated only under low-speed conditions in which the angular velocity does not exceed the threshold value.

As shown in the result of Eq. (18), the expected induced electromotive force in this study is 8.55 V, and the induced current measured in the experiment with a 1.2 Ω resistor is approximately 7.125 A. On this basis, the corresponding power is given by following equation.

$$P = VI = 60.92\,W \tag{34}$$

The comparison between the expected values and the experimental results is summarized in Table 3.

Table.3 Data comparison.

Comparison / Physical quantity	Expected	Result
$V\,[V]$	8.55V	1.56V
$I\,[A]$	7.125A	1.3A
$P\,[W]$	60.92W	2.028W

The factors presumed to account for the discrepancy between the expected and observed results are as follows

1. Conversion losses in the transformation of mechanical energy into electrical energy.
2. Energy dissipation due to friction and heat.
3. Misalignment between the magnet's rotation and the coil orientation.

Electromagnetic induction fundamentally involves the conversion of mechanical energy, arising from the relative motion between the magnet and the coil, into electrical energy. In the theoretical calculations of this study, the reduction of mechanical energy was not considered, thereby producing overestimated values. Moreover, the calculations assumed an idealized system without friction or air resistance, and neglected losses in the conversion process. Finally, while the theoretical model presupposed that the angle between the magnet and the cross-sectional area of the coil remained constant, in practice, the magnet's rotation can lead to variations in this angle, further affecting the induced electromotive force. These factors collectively explain the observed divergence between the theoretical estimates and experimental results.

7.2. Representation of Improved Study

An improved version of this research can be designed as follows. In the present experiment, the central axes of the magnet and coil were not perfectly aligned, potentially leading to reductions in the induced electromotive force. To address this, a guiding fixture to stabilize the passage of the coil is necessary. Furthermore, in this study, a single diode was employed for each coil to block reverse currents. By instead adopting a bridge rectifier circuit, reverse currents could also be rectified and utilized, thereby increasing the power output of the energy harvester and ensuring a more uniform performance.

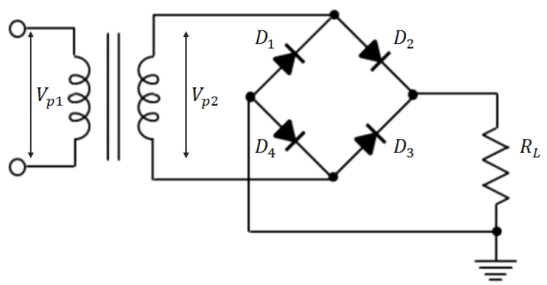

Figure.10 Bridge rectifier circuit..

The energy-harvesting generator fabricated in this study is located within the wheel itself, thereby distinguishing it from previous approaches. Consequently, if integrated with other generators applied externally to the wheel or suspension, the system could achieve higher overall efficiency while also supplementing power generation under low-speed conditions, where conventional generators typically underperform.

8. Acknowledgement

■ Reference

[1] George E. Halkos, Eleni-Christina Gkampoura, “Reviewing Usage, Potentials, and Limitations of Renewable Energy Source,” *Energies*, vol. 13, issue. 11, 2020.

[2] M. W. Aljibory, H. T. Hashim, W. N. Abbas, “A Review of Solar Energy Harvesting Utilising a Photovoltaic-Thermoelectric Integrated Hybrid System,” IOP Conference Series: Materials Science and Engineering, vol. 1067, 2020.

[3] Chongfeng Wei, Xingjian Jing, “A comprehensive review on vibration energy harvesting: Modelling and realization,” *Renewable and Sustainable Energy Reviews*, vol. 74, pp.1-18, 2017.

[4] Heung Soo Kim, Joo-Hyong Kim, Jaehwan Kim, “A review of piezoelectric energy harvesting based on vibration,” *International Journal of Precision Engineering and Manufacturing*, vol. 12, pp.1129-1141, 2011.

[5] Wenzhou Lin, Yuchen Wei, Xupeng Wang, Kangjia Zhai, Xiaomin Ji, “Study of Human Motion Energy Harvesting Devices: A Review,” *machines*, vol. 11, issue. 10, 2023.

[6] Mohamed A. A. Abdelkareem, Lin Xu, Mohamed Kamal Ahmed Ali, Ahmed Elagouz, Jia Mi, Sijing Guo, Yilun Liu, Lei Zuo, “Vibration energy harvesting in automotive suspension system: A detailed review,” *Applied Energy*, vol. 229, pp.672-699, 2018.

[7] G. Manla, N. M. White, J. Tudor, “HARVESTING ENERGY FROM VEHICLE WHEELS,” in *Proc. IEEE Int. Solid-State Sensors, Actuators and Microsystems Conf*, Denver, USA, pp.1389-1392, 2009.

[8] Vaishak, Roopa Manjunatha, G. L. Manjunath, “Piezoelectric Energy Harvesting from Automotive Wheels,” *Springer Proceedings in Materials*, vol. 18, pp.163-178, 2022.

[9] Lei Sun, Linqiang Feng, Bowen Yang, Jingjun Lin, Baojun Yu, Jin Li, Lipeng He, “Design and Study of a Rotating Piezoelectric Energy Harvester with Dual Excitation Modules,” *Journal of Electric Materials*, vol. 53, pp.4197-4213, 2024.

[10] Yunshun Zhang, Rencheng Zheng, Keisuke Shimono, Tsutomu Kaizuka, Kimihiko Nakano, “Effectiveness Testing of a Piezoelectric Energy Harvester for an Automobile Wheel Using Stochastic Resonance,” *Sensors*, vol. 16, issue. 10, 2016.

[11] Vishal M, Santhosh shankar A, “Piezoelectric energy harvesting from automotive tyres,” *Sensors*, vol. 16, issue. 10, 2016.